The LTE simulation on decaying arc plasmas in various arc quenching gases in a model circuit breaker

メタデータ	言語: eng
	出版者:
	公開日: 2017-10-03
	キーワード (Ja):
	キーワード (En):
	作成者:
	メールアドレス:
	所属:
URL	http://hdl.handle.net/2297/45474

The LTE Simulation on Decaying Arc Plasmas in Various Arc Quenching Gases in a Model Circuit Breaker

Kosuke Murai[1], Tomoyuki Nakano[1], Yasunori Tanaka[1], Yoshihiko Uesugi[1], Tatsuo Ishijima[1]
[1]Kanazawa University, Kakuma, Kanazawa 920-1192, Japan

Tatsuro Shiraishi[2], Takahiro Shimizu[2], Kentaro Tomita[2]
[2]Kyusyu University, Kasuga 816-8580, Japan

Katsumi Suzuki[3]
[3]Tokyo Denki University, Senjuasahi, Adachi 120-8551, Japan

Takayasu Fujino[4]
[4]University of Tsukuba, Tennodai, Tsukuba 305-8577 120-8551, Japan

Abstract—The present report describes numerical thermofluid simulation results of various gas arcs in a nozzle space at atmospheric pressure on the assumption of local thermodynamic equilibrium condition. It is crucial to investigate fundamentals on arc extinction phenomena by numerical simulation approach as well as experimental approach. The SF_6, Ar, CO_2 and N_2 arcs in our experimental setup were treated for the present calculation because we can accurately control the voltage and arc current in our experimtants and we can perform accurate electron density measurements for fundamental investigation and comparison. Two-dimensional temperature distributions in various gas-blast arcs were calculated in a steady state at a direct current of 50 A. Furthermore, transient temperature distributions in these arcs were computed under free recovery condition. Then, we calculated transient responses under free recovery condition by using calculated results in the steady state. The calculated arc voltage in the steady state and the transition of electron density under free recovery condition were compared with those obtained by laser Thomson scattering method in our experiments.

Index Terms—gas circuit breaker, SF_6, arc, thermofluid simulation, alternative gas

I. INTRODUCTION

Sulfur hexafluoride (SF_6) gas is widely used as an arc quenching medium in a high-voltage gas circuit breaker (GCB) because SF_6 has 100 times higher arc interruption performance than air. However, it has 22,800 times higher global warming potential (GWP) than CO_2, and thus it has been specified as one of gases to reduce its release amount. From this reason, it is greatly desired to reduce the amount of SF_6 use in GCBs as less as possible. To reduce use of SF_6 amount, much effort has been made to search for alternative gases as an arc quenching media [1], [2]. The candidates has been high pressure CO_2, N_2, CF_3I and their gas mixtures. However, these gases or gas mixtures have still much lower arc interruption performance compared to SF_6. In addition, arc interruption phenomena are markedly complex because there include various underlying physics such as arc

plasma, high intensity radiation and absorption, turbulent flow, interactions with the electrode and nozzle materials and so on, involving high gas-temperature and high speed gas flow. Furthermore, he success or failure of interruption is determined in very short time of the order of μs. For this reason, it is crucial to study the arc extinction phenomena in detail again with both accurate experimental approach [1], [3] and accurate numerical simulation approaches [2], [4], [5], [6].

We have conducted a fundamental study for elucidation of the arc extinction phenomena in both numerical and experimental approaches. In our previous experimental approach, we established a new system of decaying arc plasma using a direct-current power source and an insulated gate bipolar transistor (IGBT). This experimental system can accurately control the supplied current and applied voltage to arc plasmas in a gas flow. Using this system, we observed the fundamental behaviors of arc discharges in SF_6, Ar, and Ar/SF_6 gas flow in a nozzle space in a steady state, and also under free recovery condition with a high speed video camera [7]. In addition, decaying processes in the electron density in SF_6, Ar, and Ar/SF_6 arc plasmas were also accurately measured using a laser Thomson scattering method [8]. On the other hand, we also performed numerical simulation approach, in which Arc plasmas in SF_6, Ar, and Ar/SF_6 gas flow in a nozzle space were numerically simulated on the LTE assumption [9]. Other advanced numerical modeling for SF_6 arcs has been also made with consideration of non-equilibrium effects [10].

In this paper, we calculated two-dimensional temperature distribution of arc plasmas in various gas species in a steady state and under free recovery condition as the first fundamental approach. The model adopted here assumes local thermodynamic equilibrium (LTE) condition for arc plasmas. For comparison and fundamental investigation of alternative gases, SF_6, Ar, CO_2 and N_2 were used as flow gases. The arc voltage in a steady state and the transient electron density around the nozzle throat under
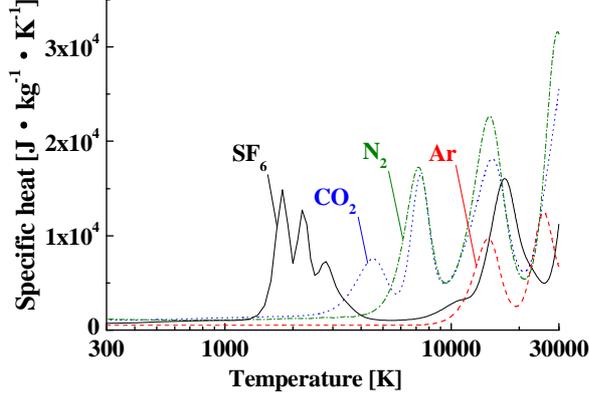
Fig. 1. Specific heat of SF_6, Ar, CO_2 and N_2 at a pressure of 0.1 MPa.

Fig. 2. Thermal conductivity of SF_6, Ar, CO_2 and N_2 at a pressure of 0.1 MPa.

free recovery condition were also calculated in numerical simulation. The calculated results were compared with experimental results to confirm the dominant physics in decaying arcs.

II. THERMODYNAMIC AND TRANSPORT PROPERTIES OF VARIOUS GASES

The numerical simulation for arc plasmas requires the thermodynamic and transport properties of the thermal plasmas and gases. In this calculation, the thermodynamic and transport properties of SF_6, Ar, CO_2 and N_2 were computed in the temperature range of 300 - 30,000 K. Equilibrium compositions of those gases were calculated by minimization of Gibb's free energy of a system. Using equilibrium composition calculated, their thermodynamic properties were computed such as the mass density, enthalpy, and specific heat at constant pressure. The transport properties such as electrical conductivity, thermal conductivity and viscosity were computed by the first order approximation of Chapman-Enskog method together with collision integrals between the species considered. Figures 1 and 2 show the specific heat and thermal conductivity, respectively, of SF_6, Ar, CO_2 and N_2 at atmospheric pressure 0.1 MPa. As for SF_6, the peculiar peaks are seen in the specific heat and thermal conductivity at temperatures around 1800, 2000 and 2200 K. The thermal dissociation/association reactions from SF_6 to SF_4, SF_4 to SF_2 and SF_2 to SF cause this effective increase in these properties. The other gases have also thier peculiar peaks due to the thermal dissociation/association reactions, respectively.

III. MODELING OF THE ARC PLASMA IN A NOZZLE SPACE

The numerical modeling for arcs in SF_6, Ar, CO_2 and N_2 gas flow was conducted under the following nine assumptions only for simplicity. (1) The calculation domain has axisymmetric structure. (2) The arc plasma is in local thermodynamic equilibrium (LTE) condition. (3) The flow is laminar flow, thus turbulent effect is neglected. (4) The arc plasma is optically thin. (5) The phenomena on the electrode surface such as electron emission, ion bombardment are neglected. (6) The electric field has only axial direction component. (7) We neglect density fluctuations caused by pressure fluctuations in a steady state. (8) Ablation effects of the electrodes and nozzle are neglected. (9) We consider heat conduction inside the electrodes and nozzle.
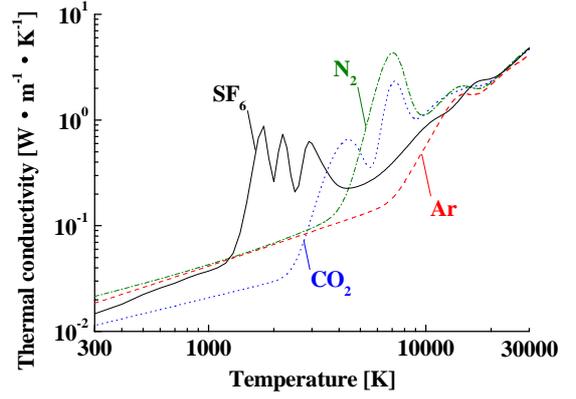
A. Governing equations

The present model assumes that the arc plasma is governed by the following fluid equations.

Mass conservation equation:

$$\frac{\partial \rho}{\partial t} + \nabla \cdot (\rho \boldsymbol{u}) = 0 \tag{1}$$

Momentum conservation equation:

$$\frac{\partial (\rho \boldsymbol{u})}{\partial t} + \nabla \cdot (\rho \boldsymbol{uu}) = -\nabla p + \nabla \cdot \boldsymbol{\tau} + \sigma \mu_0 (\boldsymbol{E} \times \boldsymbol{H}) \tag{2}$$

Energy conservation equation:

$$\frac{\partial (\rho h)}{\partial t} + \nabla \cdot (\rho \boldsymbol{u} h) = \nabla \cdot (\frac{\kappa}{C_p} \nabla h) + \frac{Dp}{Dt} + \sigma |\boldsymbol{E}|^2 - P_{rad} \tag{3}$$

Law of Ohm:

$$E_z = \frac{I}{\int_0^\infty 2\pi \sigma r dr} \tag{4}$$

Law of Ampare:

$$H_\theta = \frac{1}{r} \int_0^r \sigma E_z \xi d\xi \tag{5}$$

where t : time, z : axial position, r : radial position, u : axial gas flow velocity, v : radial gas flow velocity, ρ : mass density, p : pressure, h : enthalpy, κ : thermal conductivity, C_P : specific heat at constant pressure, P_{rad} : radiation loss, σ : electrical conductivity, μ_0 : magnetic permeability $\boldsymbol{E}$: electric field, $\boldsymbol{H}$: magnetic field, $\frac{D}{Dt} = \frac{\partial}{\partial t} + \boldsymbol{u} \cdot \nabla$: Lagrangian derivative.
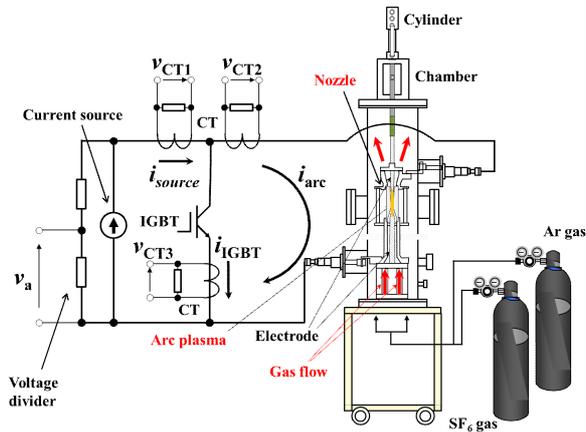
Fig. 3. Experimental setup
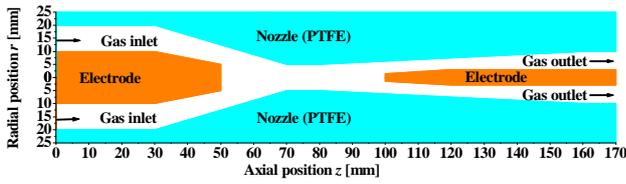
Fig. 4. Calculation domain.

Fig. 5. Calculation mesh.

(a) SF$_6$

(b) Ar

(c) CO$_2$

(d) N$_2$

Fig. 6. Two-dimensional temperature distribution of arc in a steady state in SF$_6$, Ar, CO$_2$ and N$_2$ gas flow.

B. Calculation domain and condition

Figure 3 shows the arc device and electric circuit used in the experiment [7]. In the present calculation in this paper, the arc device used in the experiment were treated. Figure 4 shows the two-dimensional calculation domain, which corresponds to the cross section of the nozzle space in the arc device shown in Fig. 3. The calculation domain is 170 mm × 50 mm. The electrodes having different diameters are located with a distance of 50 mm. The arc plasma is assumed to be formed between the electrodes. Gas is supplied at the inlet at an axial position z=0 mm, and the gas flows out freely at an axial position z=170 mm. The nozzle throat inlet is located at 20 mm distance from the upstream electrode tip. The nozzle throat has a diameter of 10 mm and a length of 10 mm. From our experiment, we found that a nozzle throat inlet was one of the key positions to decay arc plasmas in the nozzle. Figure 5 shows the calculation grid. The calculation domain is divided non-uniformly into 170 × 153 grids.

We assume that the nozzle was made of polytetrafluoroethylene (PTFE), the same material as in the experiment. The temperature at the gas inlet z=0 mm was fixed at 300 K, and the pressure at one point of the gas outlet was fixed to 0.1 MPa. For comparison and fundamental investigation among alternative gases, we selected SF$_6$,

Ar, CO$_2$ and N$_2$ as flow gases in numerical simulation as well as in the experiment. Ar is noble gas and is widely used for plasma application such as welding arcs etc. The CO$_2$ and N$_2$ have been investigated for alternative gases. The gas flow velocity at the gas inlet was set to 1.768 m/s. The gas flow velocity of 1.768 m/s is the value deduced from the gas flow rate of 100 L/min in our experiment. Therefore, its value was adopted in this calculation for comparison with experimental results.

First, we calculated the spatial distributions of gas flow and temperature fields in arc plasmas at an arc current of DC 50 A in a steady state. After that, transient distribution of gas flow and temperature fields in arc plasmas under free recovery condition were calculated using the gas flow and temperature distributions in the steady state as initial values. The free recovery condition was realized by changing current value from DC 50 A to 0 A on 0 μs. For the calculation, the SIMPLE algorithm was adopted.

IV. The two-dimensional temperature distributions of arc plasmas in a steady state

A. The difference between various gases

Figures 6 shows the two-dimensional temperature distribution of arc in a steady state in cases of SF$_6$, Ar, CO$_2$ and N$_2$, respectively. These figures indicate that the
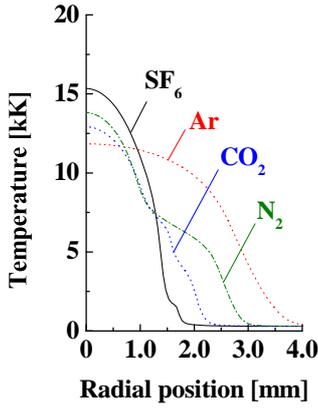
Fig. 7. Radial temperature distribution at $z = 70$ mm in SF_6, Ar, CO_2 and N_2 gas flow. (Gas flow velocity at inlet : 1.768 m/s)

Fig. 8. Numerically calculated arc voltage in the steady state

Fig. 9. Experimentally obtained arc voltage in the steady state

SF_6 arc becomes most narrow in radial direction among the four kinds of gases. For example, if we define the arc radius by the electrical conductivity above 1000 S/m in radial direction in this report, the SF_6 arc plasma has a 0.34 times smaller radius than the Ar arc. This arc shrinkage arises from energy consumption for effective dissociation of SF_6 into SF_4 or SF_2 around 2,000 K. For every gas kind treated here, the arc plasma is thinner around nozzle throat inlet $z=70$ mm. This is because of higher convection loss due to gas flow around the nozzle throat. Thus, we focus on the radial temperature distribution at the nozzle throat here. Figure 7 shows the radial temperature distributions around $z=70$ mm in order to compare the arc radius easily. As seen in Fig. 7, while Ar arc has the wide high-temperature region above 5,000 K, SF_6 arc has remarkably narrow high-temperature region. As a result, the axial temperature of thre SF_6 arc reaches to 15,000 K. As for CO_2, the arc shrunk not so much strongly as SF_6. The temperature of N_2 arc is similar to that of CO_2 arc in a radial position from $r=0$ mm to 1.5 mm. On the other hand, N_2 arc has higher than CO_2 arc in a radial position from $r=1.5$ mm to 3.0 mm. This is because N_2 does not has any dissociation reaction while CO_2 has dissociation reactions around such temperature of 2,000 and 4,000 K.

B. Arc voltage in the steady state

The arc resistance is one physical parameter to indicate the arc property. The arc voltage corresponds to the arc resistance for the same current. The arc voltage is also affected by the gas kind. Figures 8 and 9 show the calculated arc voltage in the steady state and those obtained in the experiment, respectivity. Note that the arc voltage calculated here is only a column voltage without consideration of electrode fall voltages. As for the shape of nozzle, we used the PTFE nozzle for Laser Thomson scattering method in the experiment [8]. The gas flow velocity at the gas inlet was set to 1.768 m/s as the same condition to the gas flow rate of 100 L/min in our experiment for comparison. As compared Fig. 8 with 9, the calculated arc voltage of Ar arc is similar
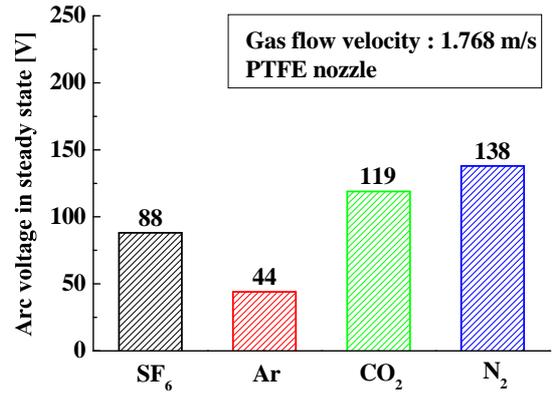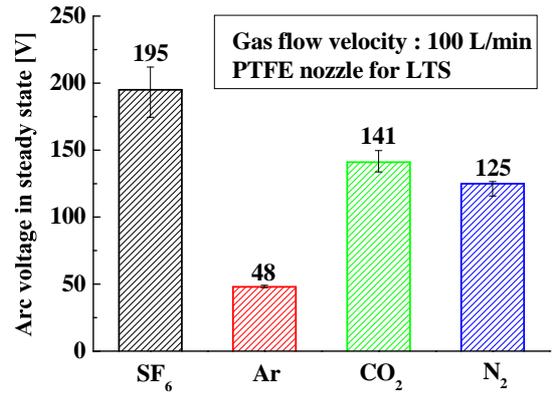
to the experimental one. However, the arc voltages of SF_6 arc and CO_2 arc in the experiment are higher in the experiment than those obtained in numerical simulation. One reason is that we neglected the electrode fall voltages on the cathode and the anode. The electrode fall voltages for SF_6 in Cu-W electrodes were measured to be 17.5 V [12]. Other reasons includes turbulent effects, electrode evaporation and non-equilibrium effects. In particular, the SF_6 arc is remarkably affected by turbulent flow because of heavy molecular weight of SF_6 (146) and then mass density. Therefore, the SF_6 arc voltage would be obtained in calculation considering turbulent effect.

V. Transient temperature distribution under free recovery condition in various gas arcs

We calculated the transient temperature distribution of various gas-blast arcs under free recovery condition to study decaying arc behaviors in various gases. Figure 10 shows transition of the arc temperature distribution of arc from $t=0$ μs to $t=100$ μs in SF_6 gas at atmospheric pressure. After current down from 50 A to 0 A, the arc plasma decays rapidly with time. The arc temperature decreases in a whole arc region from $t=0$ μs to $t=10$ μs. The arc temperature around the nozzle throat inlet decreases more rapidly. From $t=50$ μs to $t=100$ μs, the arc temperature decreases slowly. Figure 11 shows time variation in the temperature at an axial position $z=78$ mm,

(a) 0 μs

(b) 10 μs

(c) 20 μs

(d) 50 μs

(e) 100 μs
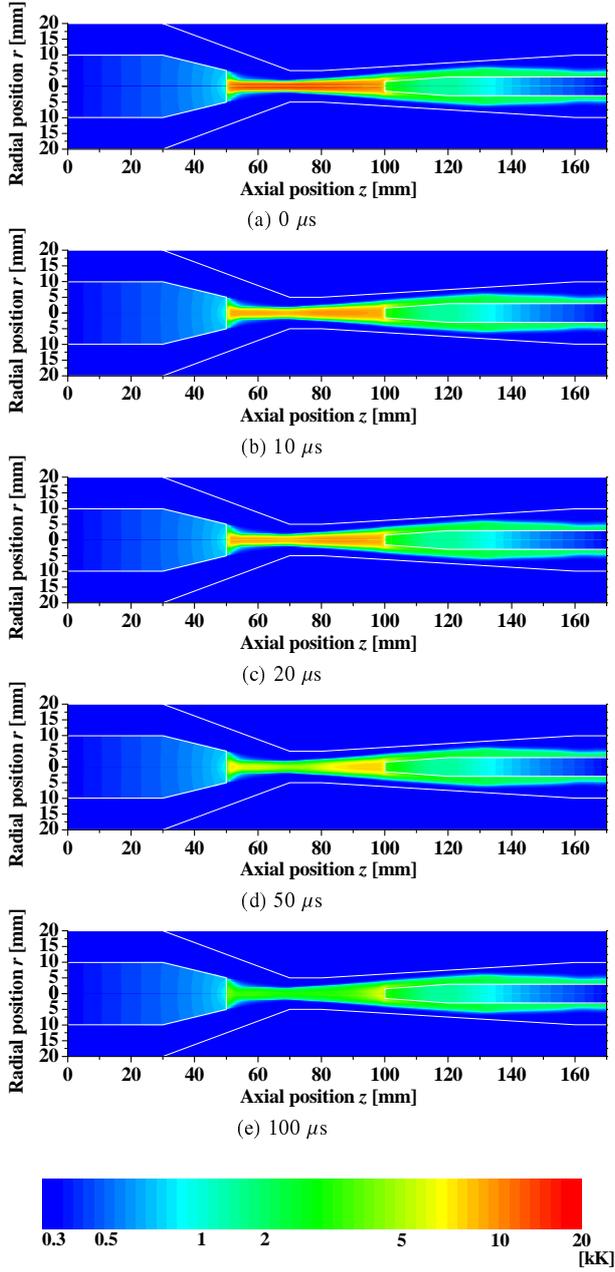
Fig. 10.   Transition of temperature distribution in 100%SF_6 gas arcs (Gas flow velocity at inlet : 1.768 m/s)

Fig. 11.   Transitions of the temperature in SF_6, Ar, CO_2 and N_2 gas-blast arcs at axial position z=78 mm
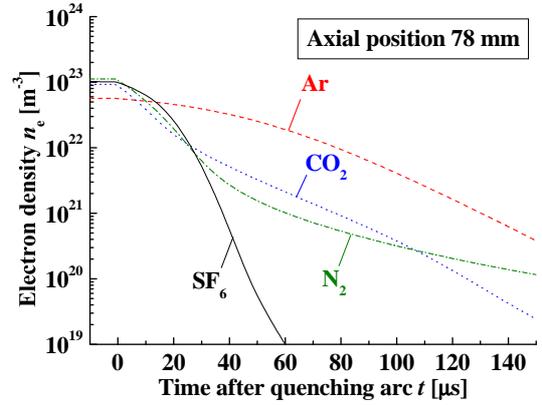
Fig. 12.   Time variation in electron density (numerical simulation)
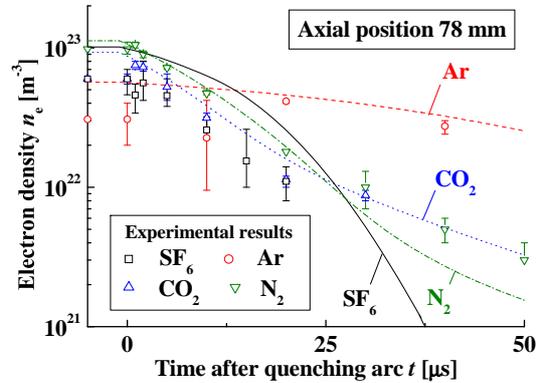
Fig. 13.   Comparison of electron density in numerical simulation with experimental result

the nozzle throat outlet, in SF_6, Ar, CO_2 and N_2 gas-blast arcs. This position is selected because the electron density was measured by laser Thomson scattering in the experiment, and the calculated electron density can be compared with the experimental results as described later. The figure indicates that the SF_6 arc has a remarkably fast decay in the temperature compared to the arcs in other gases. The SF_6 arc has strong radial temperature gradient from its high specific heat and thermal conductivity around 1800, 2000 and 2200 K due to the thermal dissociation/association reactions of SF_6. Therefore, the rapid decay in the temperature is obtained after the input power down to zero. In contrast to SF_6 arc, the Ar arc remains to have temperatures above 9,000 K and has high conductive property even at t=100 μs. The CO_2 arc

temperature also decreases rapidly from t=0 μs to t=20 μs, but the arc temperature decreases more slowly from t=20 μs compared to those in SF_6. This similar tendency is seen in N_2 arc as well.

VI. COMPARISON OF ELECTRON DENSITY IN NUMERICAL SIMULATION WITH EXPERIMENTAL RESULT UNDER FREE RECOVERY CONDITION

Figure 12 shows transitions of the electron density at the nozzle throat outlet z=78 mm on the axis under free

recovery condition from $t=0$ μs to $t=150$ μs, which is estimated by the present LTE numerical simulation. As indicated in Fig. 12, the electron density in a SF_6 gas-blast arc drops markedly from 1×10^{23} m^{-3} to 6×10^{19} m^{-3} in $t=50$ μs. On the other hand, Ar arc keeps high electron density above 2×10^{22} m^{-3} at 50 μs after current down to 0 A. At 150 μs, SF_6 residual arc has the lowest electron density, and then the second lowest electron density is in CO_2. To compare with the numerically obtained electron density, transition in the electron density is plotted with calculated result in Fig. 13, which was obtained by laser Thomson scattering method in the experiment from $t=0$ μs to $t=50$ μs [8]. As seen in these figures, the calculated electron density decays in CO_2, N_2 and Ar are similar to the experimental ones. The electron density in SF_6 arcs clearly decreases much more rapidly than Ar arcs in both experimental and calculation results. However, there is still some difference in the electron density between the calculation results and experimental results in gases. In numerical simulation result, the SF_6 gas-blast arc has a higher electron density and a slower decay than those in the experimetnal result. These may be due to neglected underlying physics such as turbulent effects and chemically non-equilibrium effects. Our future work should consider the above more detailed physics.

VII. Summary

In this paper, we performed a numerical simulation for arc plasma in gas flow in a nozzle space under free recovery condition on the LTE assumption. The arcs in our experimental setup were treated for calculation because we can accurately control the voltage and arc current in the experimtants and we can perform accurate electron density measurements. For comparison and fundamental investigation of alternative gases, SF_6, Ar, CO_2 and N_2 were selected as gas flow as with in experiment. First, we calculated the temperature distribution of arc in those gas flows in the steady state. Then, transient responses of the arc temperature were calculated under free recovery condition. We compared the arc voltage in the steady state and transition of electron density under free recovery condition with experimental ones. As the results, the SF_6 arc has a fast decay in the temperature and the electron density compared to the arcs with other gases. Especially, this tendency is shown remarkably in contrast to Ar arc and this is similar to the experimental result. However, there is a difference between the calculation result and experimental result such as the arc voltage andthe electron density decay especially in SF_6 gases. Thus, the arc model would be improved considering more detailed physics such as turbulent effects and non-equilibrium effects.

References

[1] P. C. Stoller, M. Seeger, A. A. Iordanidis, G. V. Naidis: "CO_2 as an arc interruption medium in gas circuit breakers" *IEEE Trans. Plasma Sci.*, Vol.41, No.8, 6522876, pp. 2359-2369 (2013)

[2] Y. Tanaka, X. Song, Y. Uesugi, S. Kaneko, S. Okabe: "Numerical simulation on quenching process of carbon dioxide arcs with hydrogen gas inclusion in different nozzle shapes", *IEEJ Trans. PE*, Vol.133, No.11, pp. 895-902 (2013)

[3] Y. Inada, S. Yamagami, S. Matsuoka, A. Kumada, H. Ikeda, K. Hidaka: "Simultaneous imaging of two-dimensional electron density and air-flow distribution over air-blast decaying arc", *J. Phys. D: Appl. Phys*, Vol.47, No.32, 325204 (2014)

[4] W. Z. Wang, J. D. Yan, M. Rong, Y. Wu, J. W. Spencer: "Investigation of SF_6 arc characteristics under shock condition in a supersonic nozzle with hollow contact", *IEEE Trans. Plasma Sci.*, Vol.41, No.4, 6482262, pp. 915-928 (2013)

[5] D. Biswas, T. Jimbo, K. Udagawa, T. Shinkai, K. Suzuki: "Studies on fluid-plasma interaction associated with basic gas blast characteristics based on a high-order LES turbulence model", *IEEJ Trans. PE*, Vol.133, No.5, pp. 417-423 (2013)

[6] Y. Tanaka, K. Suzuki: "Development of a chemically nonequilibrium model on decaying SF_6 arc plasmas", *IEEE Trans. Power Delivery*, Vol.28, No.4, 6545389, pp. 2623-2629 (2013)

[7] Y. Tanaka, T. Nakano, K. Tomita, T. Fujino, K. Suzuki: "Experimental Investigation on Decaying Arc Behaviors in Alternative Gas Flow using Semiconductors", *Joint Conf. IWHV2014*, ED-14-084, SP-14-040, HV-14-096(2014)

[8] K. Tomita, D. Gojima, K. Nagai, K.Uchino, R. Kamimae, Y.Tanaka, K.Suzuki, T.Iijima, T. Uchii, T.Shinkai: "Thomson scattering diagnostics of decay processes of Ar/SF6 gas-blast arcs confined by a nozzle", *J. Phys. D: Appl. Phys.*, **46**, 382001 (2013)

[9] K. Murai, Y. Tanaka, T. Nakano, K. Tomita, T. Fujino, K. Suzuki, "The LTE Thermofluid Simulation of Ar/SF6 Gas-Blast Arcs in a Nozzle Space in an Arc Device", *Joint Conf. IWHV2014*, ED-14-086, SP-14-042, HV-14-098(2014)

[10] Y.Tanaka, K.Suzuki, "Development of a chemically non-equilibrium model on decaying SF6 arc plasmas", *IEEE Trans. Power Delivery* , Vol.28, Issue 4, pp.2623-2629(2013)

[11] A Gleizes, Y Cressault, and Ph Teulet, "Mixing rules for thermal plasma properties in mixtures of argon, air and metallic vapours", *Plasma Sources Sci. Technol.*, **19**, 055013 (2010)

[12] Y. Yokomizu, T. Matsumura, R. Henmi, Y. Kito: "Total voltage drops in electrode fall regions of SF_6, argon and air arcs in current range from 10 to 20 000 A", *J. Phys. D: Appl. Phys.*, Vol.29, No.5, pp. 1260-1267 (1996)